REVIEW

Activation of PPARδ: from computer modelling to biological effects

Shirin Kahremany[1], Ariela Livne[2], Arie Gruzman[1], Hanoch Senderowitz[1] and Shlomo Sasson[2]

[1]*Division of Medicinal Chemistry, Department of Chemistry, Faculty of Exact Sciences, Bar-Ilan University, Ramat-Gan, Israel, and* [2]*Department of Pharmacology, Institute for Drug Research, School of Pharmacy, Faculty of Medicine, The Hebrew University of Jerusalem, Jerusalem, Israel*

Correspondence
Professor Shlomo Sasson, Department of Pharmacology, Institute for Drug Research, School of Pharmacy, Faculty of Medicine, The Hebrew University of Jerusalem, Faculty of Medicine, Jerusalem 91120, Israel. E-mail: shlomo.sasson@mail.huji.ac.il; Professor Hanoch Senderowitz, Division of Medicinal Chemistry, Department of Chemistry, Faculty of Exact Sciences, Bar-Ilan University, Ramat-Gan 52900, Israel. E-mail: hsenderowitz@gmail.com

PPARδ is a ligand-activated receptor that dimerizes with another nuclear receptor of the retinoic acid receptor family. The dimers interact with other co-activator proteins and form active complexes that bind to PPAR response elements and promote transcription of genes involved in lipid metabolism. It appears that various natural fatty acids and their metabolites serve as endogenous activators of PPARδ; however, there is no consensus in the literature on the nature of the prime activators of the receptor. *In vitro* and cell-based assays of PPARδ activation by fatty acids and their derivatives often produce conflicting results. The search for synthetic and selective PPARδ agonists, which may be pharmacologically useful, is intense. Current rational modelling used to obtain such compounds relies mostly on crystal structures of synthetic PPARδ ligands with the recombinant ligand binding domain (LBD) of the receptor. Here, we introduce an original computational prediction model for ligand binding to PPARδ LBD. The model was built based on EC_{50} data of 16 ligands with available crystal structures and validated by calculating binding probabilities of 82 different natural and synthetic compounds from the literature. These compounds were independently tested in cell-free and cell-based assays for their capacity to bind or activate PPARδ, leading to prediction accuracy of between 70% and 93% (depending on ligand type). This new computational tool could therefore be used in the search for natural and synthetic agonists of the receptor.

Abbreviations
ALPHA, amplified luminescent proximity homogeneous assay; CARLA, co-activator-dependent receptor ligand assay; DBD, DNA binding domain; LBD, ligand binding domain; LIC, ligand-induced complex formation assay; MUFA, monounsaturated fatty acids; NTD, N-terminal domain; PPRE, PPAR response elements; PUFA, polyunsaturated fatty acids; RMSD, root mean squared deviation; RXR (also known as NR2B receptors), retinoid X receptor; SFA, saturated fatty acids; SP, scintillation proximity competition assay; TR-FRET, time resolved-fluorescence resonance energy transfer

Tables of Links

TARGETS
PPARα
PPARδ
PPARγ
Retinoic acid receptors
Retinoid X receptors (RXR)
RXRα

LIGANDS			
15d-$\Delta^{12,14}$-PGJ$_2$	EPA	Lauric acid	PGD$_2$
12-HpETE	ETYA	Linoleic acid	PGD$_3$
15-HpETE	Fenofibrate	LTA$_4$	PGE$_1$
α-linolenic acid	Gemfibrozil	LTB$_4$	PGE$_2$
γ-linolenic acid	GW0742	LTC$_4$	PGF$_{1\alpha}$
Bezafibrate	GW2433	LXA$_4$	PGF$_{2\alpha}$
Capric acid	GW501516	LXB$_4$	PGI$_2$
Cicaprost	IL-6	Myristic acid	Probucol
Ciprofibrate	IL-8	Oleic acid	Ragaglitazar
Clofibrate	Iloprost	Palmitic acid	Stearic acid
DHA	L-165041	PGA$_2$	Wy14643

These Tables list key protein targets and ligands in this article which are hyperlinked to corresponding entries in http://www.guidetopharmacology.org, the common portal for data from the IUPHAR/BPS Guide to PHARMACOLOGY (Pawson *et al.*, 2014) and are permanently archived in the Concise Guide to PHARMACOLOGY 2013/14 (Alexander *et al.*, 2013).

Introduction

The PPAR family

PPARs are ligand-activated transcription factors of the nuclear hormone receptor superfamily. Peroxisome proliferation in rat liver treated with the anti-hyperlipidaemic compound clofibrate was reported over 40 years ago (de Duve, 1969). Subsequently, several other compounds with similar effects were identified and were collectively termed peroxisome proliferators. Issemann and Green cloned the first member of the family from rat liver, and in 1990 coined the term 'peroxisome proliferator-activated receptor' (Issemann and Green, 1990). Two other members of the family were identified in 1992 and the group now consists of three major subtypes: PPARα, PPARδ and PPARγ (Dreyer *et al.*, 1993). These receptors regulate major metabolic pathways, including carbohydrate utilization, fatty acid oxidation and lipogenesis (Wagner and Wagner, 2010). They form heterodimers with members of the retinoic acid receptor (RXR) family and subsequently interact in a stereospecific manner with PPAR response elements (PPRE) in DNA to assemble active transcriptional complexes (Wahli and Michalik, 2012). PPRE sequences are composed of double hexameric motifs, separated by a short spacer sequence and organized in a direct, inverted or everted manner (Kumar and Thompson, 1999). PPARα is predominantly expressed in the liver and primarily regulates lipid metabolism (Pyper *et al.*, 2010). PPARγ is mostly expressed in adipose tissues and controls adipogenesis and carbohydrate metabolism (Astapova and Leff, 2012).

Roles of PPARδ in the regulation of glucose and lipid metabolism

The role of the ubiquitously expressed PPARδ in the regulation of physiological and pathological processes in different tissues have been intensely investigated (Coll *et al.*, 2009; Ehrenborg and Krook, 2009; Lee *et al.*, 2009; Wagner and

Wagner, 2010; Wolf, 2010; Ehrenborg and Skogsberg, 2013; Skerrett *et al.*, 2014). The regulation of lipid and glucose metabolism is considered a major function of PPARδ (Coll *et al.*, 2009). For instance, it orchestrates the expression of genes involved in lipid metabolism in mature adipocytes (Wolf, 2010). Other studies have shown that PPARδ activation improves the plasma lipid profile in humans and in primates (Oliver *et al.*, 2001; Wallace *et al.*, 2005; Sprecher *et al.*, 2007; Riserus *et al.*, 2008; Thulin *et al.*, 2008) and significantly decreases high fat diet-induced obesity in rodents (Tanaka *et al.*, 2003). In addition, PPARδ-null mice exhibited lower accumulation of lipids in adipose tissue stores (Peters *et al.*, 2000; Sprecher *et al.*, 2007). The specific PPARδ agonist GW501516 increases blood high-density lipoprotein and decreases triglyceride levels in rhesus monkeys (Oliver *et al.*, 2001) and preventes obesity in mice (Wang *et al.*, 2003). Furthermore, PPARδ activation reduces intestinal cholesterol absorption in mice (van der Veen *et al.*, 2005).

PPARδ also plays an important role in the regulation of peripheral insulin sensitivity and attenuates symptoms of the metabolic syndrome (Tanaka *et al.*, 2003; Lee *et al.*, 2006; Riserus *et al.*, 2008). Decreased lipid accumulation in skeletal muscles following PPARδ activation along with proliferation of mitochondria and a consistent increase in fatty acids oxidation in skeletal muscles were also linked to PPARδ-dependent amelioration of insulin resistance (Dressel *et al.*, 2003; Ehrenborg and Skogsberg, 2013). Similar beneficial effects of PPARδ activation were observed in insulin-resistant obese rhesus monkeys (Oliver *et al.*, 2001). Others showed that PPARδ stimulation improved glucose tolerance, lowered postprandial levels of plasma insulin and glucose, reduced hepatic glucose output by increasing glycolysis and the pentose phosphate shunt and augmented fatty acids synthesis and triglycerides content in the liver (Tanaka *et al.*, 2003; Lee *et al.*, 2006; Chen *et al.*, 2008). Conversely, PPARδ-null mice were glucose intolerant and exhibited a low metabolic rate (Lee *et al.*, 2006).

Protective role of PPARδ in the development of atherosclerosis

Active PPARδ may also prevent or delay the development of atherosclerosis. For example, treatment with the PPARδ agonist L-165041 resulted in reduced monocyte recruitment to human endothelial cells by reducing the expression of vascular cell adhesion molecule-1, the secretion of monocyte chemotactic protein-1 and of the inflammatory cytokines IL-6 and IL-8 (Rival *et al.*, 2002; Jiang *et al.*, 2009; Liang *et al.*, 2010). Furthermore, activation of PPARδ by the selective agonists GW0742 and GW501516 augmented the expression of antioxidant genes, (e.g. superoxide dismutase-1, catalase and thioredoxin), and attenuated the generation of reactive oxygen species in vascular endothelial cells (Fan *et al.*, 2008). Others suggested that activated PPARδ augmented cholesterol efflux from macrophages in atherosclerotic lesions and thereby decreased transendothelial migration of leucocyte/monocytes into the arterial wall (For review see Barish *et al.*, 2008; Piqueras *et al.*, 2009).

PPARδ protects against pathophysiological processes in the nervous system

The findings that PPARδ-deficient mice exhibited abnormal neurophysiological processes, such as decreased myelination, augmented inflammatory reactions and low score in memory tests, suggest a critical role for PPARδ in neuronal development and function (Peters *et al.*, 2000). Interestingly, CNS inflammation has been associated with increased level of inflammatory markers, astrogliosis and τ hyperphosphorylation (Barroso *et al.*, 2013). Moreover, it was the lack of PPARδ function in the brain has been linked to increased vulnerability to ischaemic insults because of defective antioxidant responses (Arsenijevic *et al.*, 2006; Pialat *et al.*, 2007). Additional data, generated from effects of selective PPARδ agonists in the brain, suggest that PPARδ activation could protect against neurodegenerative processes (Polak *et al.*, 2005; Iwashita *et al.*, 2007; Kalinin *et al.*, 2009; Paterniti *et al.*, 2010; Yin *et al.*, 2010; Martin *et al.*, 2013).

Roles of PPARδ in embryonic, organ and tissue development

Attempts to generate PPARδ knockout mouse models were difficult because of high rates of embryo lethality (Michalik *et al.*, 2001; Barak *et al.*, 2002). Yet, these models revealed important roles of PPARδ in blastocyst hatching, embryo implantation, myelination, lipid metabolism and adiposity and epidermal cell proliferation (Lim *et al.*, 1999; Peters *et al.*, 2000; Barak *et al.*, 2002; Huang *et al.*, 2007). Furthermore, PPARδ seemed also involved in morphological adaptive differentiation of various tissues, such as skeletal muscles (Ehrenborg and Krook, 2009), and the development of oxidative type I fibres (Luquet *et al.*, 2003; Wang *et al.*, 2004). Recent studies suggest that PPARδ regulates cell growth (Lee *et al.*, 2009): for instance, it increased the number and size of intestinal polyps and stimulated proliferation of vascular smooth muscle cells, pre-adipocytes and epithelial cells (Jehl-Pietri *et al.*, 2000; Hansen *et al.*, 2001; Zhang *et al.*, 2002; Gupta *et al.*, 2004; Burdick *et al.*, 2006). Importantly, several PPARδ synthetic agonists exhibited carcinogenic potential (Ehrenborg and Skogsberg, 2013).

In conclusion, because PPARδ regulates myriad cell and organ functions, it has become a desirable target for drug discovery. Development of selective PPARδ agonists for the treatment and prevention of symptoms of the metabolic syndrome attracts attention and is highly sought. Similarly, PPARδ-selective agonists with enhanced neuroprotective and anti-atherosclerotic properties are of a great interest. Yet the carcinogenic potential of PPARδ agonists should be fully investigated in order to create selective agonists devoid of this property. Therefore, PPARδ structural research, detailed analysis of ligand binding to the receptor and its activation on the basis of comprehensive structure activity relationship analysis are required to reach these goals.

The structure of PPARδ

Generally, PPARs are organized in four functional domains: the N-terminal domain (NTD), the DNA binding domain (DBD), which includes two zinc fingers, the hinge domain and the ligand binding domain (LBD) (Schmidt *et al.*, 1992). The NTD is the most varied domain among the different PPARs (Helsen and Claessens, 2014). This domain, which is relatively short, is believed to mediate ligand-independent activity by promoting protein–protein interactions with co-activators or co-suppressors and by inducing conformational modifications that allow allosteric interactions (Zieleniak *et al.*, 2008; Helsen and Claessens, 2014). Interestingly, the NTD has not yet been resolved in the full length crystal structure of PPARδ and its precise regulatory interactions remain to be resolved. The DBD is the most conserved domain among the various PPARs. Two zinc fingers form the functional core structure, where the α-helix in the first zinc finger promotes the recognition of specific sequence in the PPRE in the DNA. The second zinc finger mediates the heterodimerization with RXR (Helsen and Claessens, 2014). Other areas in the DBD further stabilize the DNA-PPAR complex by direct interactions with the minor groove of the DNA and/or alternatively by stabilizing the interactions with other partner in the dimer complex (Hsu *et al.*, 1998; Shaffer and Gewirth, 2002; Roemer *et al.*, 2006). The hinge domain, which separates the DBD from the LBD in all PPARs, contains a nuclear localization signal and amino acid side chains amenable to post-translational modifications (Anbalagan *et al.*, 2012; Clinckemalie *et al.*, 2012).

The structure of the LBD is similar among the various PPAR (Bourguet *et al.*, 1995; Renaud *et al.*, 1995): it consists of a complex of 13 α-helices and four-stranded β-sheets that form a cavity, which is markedly larger than similar cavities in other members of the nuclear receptor superfamily. The Y-like shaped LBD in PPARs is composed of 25 amino acids (Figure 1): arm-1 forms a 'tunnel' that transverses from the surface of the protein to its internal part, while arm-2 and arm-3 form a cavity. Arm-2 is considerably polar, whereas arm-1 and arm-3 are hydrophobic. Over 80% of the amino acid residues in the binding cavity are highly conserved among the three PPAR isotypes, including four polar residues in arm-2, which form critical hydrogen bonds with polar moieties (predominantly carboxylic acids) of ligands. Correspondingly, PPAR ligands are usually characterized by the presence of a polar moiety in a predominantly non-polar molecule (Zoete *et al.*, 2007). Ligand binding selectivity to the various PPARs is conferred by subtle modifications in the
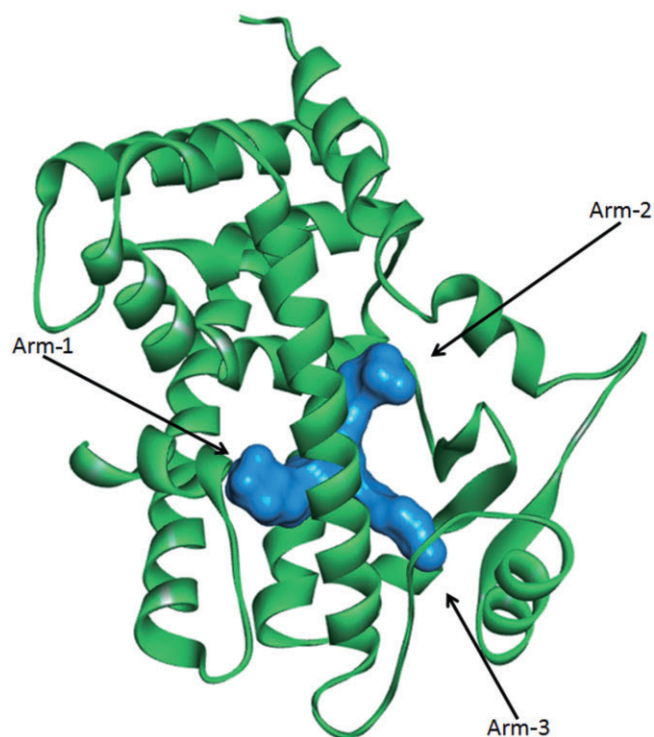
Figure 1
PPARδ crystal structure with the cavity in the ligand binding site (bkue surface). PDB code: 3GWX.

structure of their LBD (Batista *et al.*, 2012; Carrieri *et al.*, 2013). It has been shown that a single amino acid mutation in the LBD can dramatically change ligand recognition by the receptor (Xu *et al.*, 1999). The large volume of the binding cavity allows several binding options (dynamic binding equilibrium) of the lipophilic domain of ligands in the LBD, as was documented for the interaction of eicosanoic acid with the LBD PPARs (Xu *et al.*, 2001) or for ragaglitazar with PPARα/γ (Ebdrup *et al.*, 2003). Interestingly, arm-1 forms a very narrow tunnel in PPARδ LBD, which restricts the entry of compounds with bulky moieties near the polar head. This structure eliminates the binding of various PPARs α/γ ligands to the PPARδ LBD (Xu *et al.*, 1999). This structure also explains the relatively small number of known ligands to PPARδ in comparison with the two other isotypes. For instance, the bulky acidic head group in thiazolidinediones permits their binding interaction with PPARγ but not with PPARδ. Yet the relatively small phenoxyacetic acid moiety in the PPARδ agonist GW501516 fits well the narrow entry tunnel to the LBD (Oliver *et al.*, 2001).

PPARδ activation

The current hypothesis of PPAR activation claims that the binding of a ligand to the LBD triggers conformational changes in the entire receptor. Such changes that occur in helix 12 of the LBD enable interactions of co-activator molecules (e.g. steroid receptor co-activator-1) with the receptor (Kallenberger *et al.*, 2003). These conformational changes also increase the strength of the binding interaction between

PPARs and their cognate partner RXR to form active dimers that interact with PPRE in gene promoters (Okuno *et al.*, 2001). The fact that PPARs have significant constitutive activity in the total absence of ligands and co-activators indicates that the classical ligand-dependent activation of PPARs is not exclusive (Issemann and Green, 1990; Hallenbeck *et al.*, 1992).

This review focuses on ligand binding selectivity and subsequent activity of PPARδ. The human PPARδ is made of 441 amino acids that are organized in the classical NTD (aa 1–70), DBD (aa 71–145), which includes two zinc fingers (aa 74–94 and 111–133), the hinge domain (aa 146–254) and the LBD (aa 254–441) (Schmidt *et al.*, 1992). The secondary structure of the protein consists of 10 β-strands and 15 α-helices. While a full crystal structure of PPARγ has been recently reported (Chandra *et al.*, 2008), most structural information on PPARδ is restricted to analysis of LBD and hinge domain crystals (Fyffe *et al.*, 2006).

It has been shown that certain saturated, mono-unsaturated and polyunsaturated fatty acids (SFA, MUFA and PUFA) and eicosanoids and prostaglandins activate PPARδ (Benetti *et al.*, 2011). Recently, we have reported that 4-hydroxynonenal (4-HNE) and 4-hydroxydodecadienal (4-HDDE), the peroxidation products of PUFA, activate PPARδ in cultured endothelial cells and pancreatic β-cells (Riahi *et al.*, 2010; Cohen *et al.*, 2011b; 2013). The mechanism by which these two 4-hydroxyalkenals activate PPARδ is unclear. These chemically reactive aldehydes avidly form covalent bonds with nucleophilic groups of amino acids (i.e. histidine, lysine, arginine or cysteine). Yet it has been reported that steric hindrance prevents 4-HNE covalent interaction with histidine residues in the LBD of PPARδ (Coleman *et al.*, 2007).

PPARδ activators

The following methods were employed by different groups to study ligand binding interactions with PPARδ: co-activator-dependent receptor ligand assay (CARLA) (Krey *et al.*, 1997), ligand-induced complex formation assay (LIC) (Forman *et al.*, 1997), scintillation proximity competition assay (SP) (Xu *et al.*, 1999), time resolved-fluorescence resonance energy transfer (TR-FRET) (Naruhn *et al.*, 2010) and amplified luminescent proximity homogeneous assay (ALPHA) (Jin *et al.*, 2011).

CARLA reflects molecular consequences of ligand binding to the receptor and is based on the principle that binding of ligands to a nuclear receptor increases the binding affinity of a labelled 'broad spectrum' co-activator protein [35S]-SRC1 to the receptor complex. Principally, CARLA detects productive physical interactions between two proteins in the presence of a ligand and is not aimed at determining the association of ligands with the LBD *per se*. LIC is based on the observation that ligand-activated nuclear receptors bind to response elements in DNA as dimers. Thus, a gel shift mobility assay is employed to detect the capacity of PPAR-RXR complexes with potential ligands to interact with PPRE-containing DNA sequences. The SP competition assay uses the changes in light emission when PPARδ, immobilized on scintillant microscopic beads with radiolabelled ligand (e.g. [3H]-GW2433), interacts with test compounds. TR-FRET analysis is an integrated method that includes two fluorescent techniques: first, FRET interaction between two fluorophores, a donor and an

acceptor, which triggers energy transfer from the donor to the acceptor. Second, TRF (time resolved fluorescence) method takes advantage of the long-lived fluorophores lanthanides, which enables the elimination of non-specific signals. Briefly, Fluormone™ Pan-PPAR Green (Life Technologies, Carlsbad, CA, USA) is mixed with test compounds, followed by the addition of a mixture of the PPARδ-LBD and terbium anti-GST (glutathione-S-transferase) antibody. When the Fluormone Pan-PPAR Green is bound to the receptor, energy transfer from the terbium-labelled antibody to the tracer occurs and resolved as a high TR-FRET ratio. Competitive ligand binding to PPARδ is detected by the test compound's ability to displace the tracer and a reduced FRET signal. The ALPHA bead-based assay resolves the interactions of a fluorophore donor with its acceptor. The donor bead contains a high concentration of photosensitizers, which converts ambient oxygen to a more excited singlet state when excited at 680 nm. This bead is covered with an antibody against PPARδ. The acceptor bead is a chemiluminescer that is covered with the LBD of PPARδ. The binding interaction between the antibody and the LBD across the two beads results in singlet-induced luminescence. PPARδ ligands interfere with the binding interaction between the beads and lower the luminescence.

Using the CARLA, Krey et al. identified eicosatetraynoic acid, eicosapentanoic acid, linoleic acid, linolenic acid, 8(S)-hydroxyeicosatetraenoic [8(S)HETE] acid and bezafibrate as high-affinity ligands to the LBD of PPARδ (Krey et al., 1997). Forman et al. (1997) used LIC to compare the binding interactions of ligands with PPARδ LBD with their ability to transactivate the PPREX3-TK-LUC vector in transfected cells. Of all compounds tested, the best binding affinities were reported for carbaprostacyclin (cPGI, a synthetic analogue of PGI$_2$), followed by iloprost (another PGI$_2$ analogue), arachidonic and linoleic acid. Interestingly, the transactivation capacity of these compounds in the cell-based assay was different: arachidonic acid > cPGI > iloprost > linoleic acid. Unlike the results of the above-mentioned CARLA assay, 8(S)-HETE exhibited insignificant binding interaction with PPARδ LBD in the LIC assay and no activity in the cell-based assay. Also, eicosapentanoic acid, predicted to be an activator of PPARδ in the CARLA, lacked significant binding interactions with the LBD in the LIC assay, while exhibiting a marked transactivation capacity in the cell-based assay. Moreover, some compounds that interacted positively in the activation assay (e.g. PGA$_1$, PGA$_2$ or 15d-PGJ$_2$) lacked a significant binding interaction with the LBD. Xu et al. (1999) also tested some of these putative PPARδ ligands in the SP assay and ranked them as follows: arachidonic acid > eicosapentanoic acid > linoleic acid > linolenic acid. These findings correspond well with some of the results of CARLA and LIC assays. Interestingly, the most potent fatty acid tested in the SP assay was γ-linoleic acid. Other potent ligands were oleic acid, stearic acid, palmitic acid and palmitoleic acid. Using the TR-FRET assay, Naruhn et al. (2010) found that 15-HETE was most potent in inducing the binding of a co-activator-derived peptide to the PPARδ LBD in vitro, followed by arachidonic acid and 15-HpETE. Yet 8-HETE, 12-HETE and 12-HpETE had no significant interaction with the LBD. Using the ALPHA screen assay, Jin et al. (2011) confirmed that iloprost was bound to the LBD of PPARδ and PPARα. More studies utilizing other methods report that some of the above-mentioned compounds and prostaglandins could interact with PPARδ (Yu et al., 1995). Coleman et al. (2007) identified several arachidonic and linoleic acid metabolites (e.g. 12/15-HpETE, 15-HETE) as potent activators of PPARδ. Riahi et al. (2010) and Cohen et al. (2011b) introduced 4-hydroxyalkenals as another class of PPARδ activators. The peroxidation products of arachidonic acid, 4-HDDE and 4-HNE, transactivated PPREX3-TK-LUC in transfected vascular endothelial cells and cultured pancreatic β-cells.

Molecular modelling

Known crystal structures of PPARδ LBD-synthetic ligand complexes

In addition to the above-mentioned functional studies, there are 16 crystal structures of synthetic PPARδ ligands with PPARδ LBD listed in the Protein Data Bank (PDB) (Table 1). These data have been used to analyse the binding pocket in the LBD and to determine obligatory interactions between various synthetic PPARδ agonists, such as GW501516, GW0742 and TIPP204 (Sznaidman et al., 2003), and amino acid side chains in the LBD. Hitherto, no crystal structure of the whole monomeric PPARδ protein or its heterodimer with RXR has been reported. We decided to use the X-ray crystallographic data of the above-mentioned complexes with synthetic ligands and create an in silico model that may predict the degree of possible direct interactions of natural ligands (fatty acids and their metabolites) and other synthetic ligands with the PPARδ LBD. This model also tests the assumption that both large (e.g. long fatty acid and their metabolites) and small (e.g. hydroxyalkenals) ligands may enter and interact within the bulky cavity in the LBD.

Our model was developed based on previously published crystallographic data of 16 PPARδ LBD-ligand complexes and validated on a database of 82 compounds (SFA, MUFA, PUFA and some of their enzymatic and non-enzymatic metabolites and several synthetic compounds; see Tables 2 and 3). These were evaluated for their potential to bind to PPARδ LBD, using pharmacophore modelling and docking simulations. Because the binding site of the protein contains two histidine residues (H323, H449) that are important for ligand binding, we also examined the effect of the protonation states of these two residues on the ligand binding modes. The molecular modelling methods used for the following in silico analysis are given in the Supporting Information section.

Binding hypothesis and the pharmacophore model

Analysis of the binding modes of the 16 crystallographic ligands led to the hypothesis that PPARδ binders occupy arm-1 and arm-3 of the protein's binding site and frequently form interactions with H323, H449 or Y473. This hypothesis is in line with a previous study of PPARγ agonists (Iwata et al., 2001). This binding hypothesis was transformed into a pharmacophore model by superposing the 16 crystallographic ligands in their complex (i.e. bioactive) conformations. The resulting pharmacophore was further refined by adding

Table 1

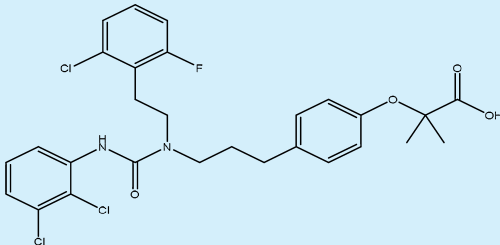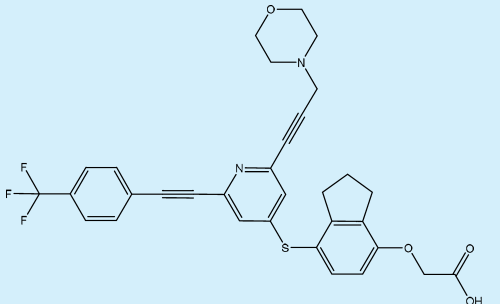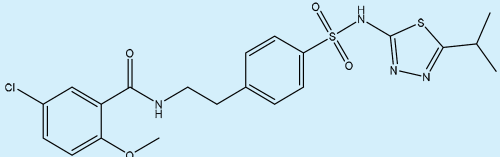Activity data for the 16 crystallographic ligands of PPARδ bound to the ligand binding domain
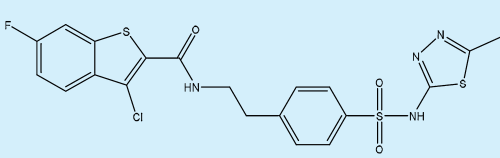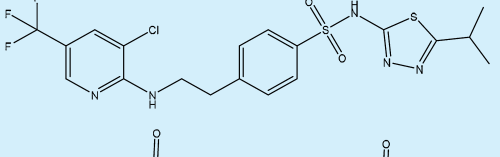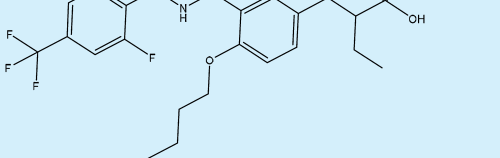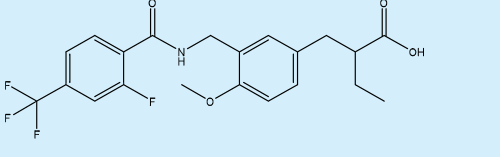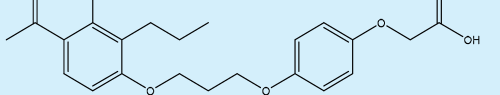
Protein Data Bank code	Ligand structure	EC$_{50}$ (nM)	Reference
1GWX		190	(Xu et al., 1999)
2Q5G		130	(Pettersson et al., 2007)
2XYJ		738	(Keil et al., 2011)
2XYW		318	(Keil et al., 2011)
2XYX		1.6	(Keil et al., 2011)
2ZNP		0.9	(Oyama et al., 2009)
2ZNQ		12	(Oyama et al., 2009)
3D5F		3800	http://www.rcsb.org/pdb/explore/explore.do?structureId=3d5f

Table 1

Continued
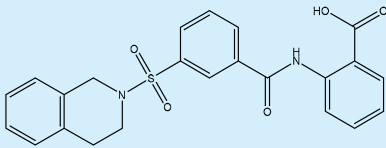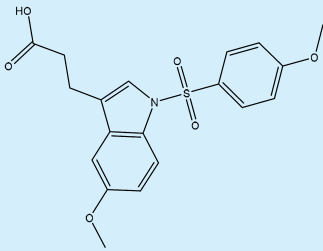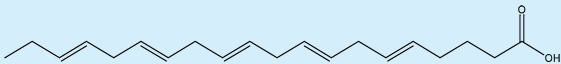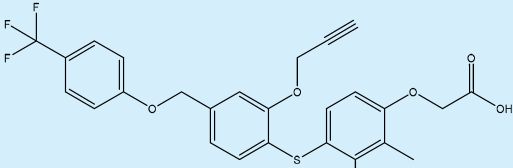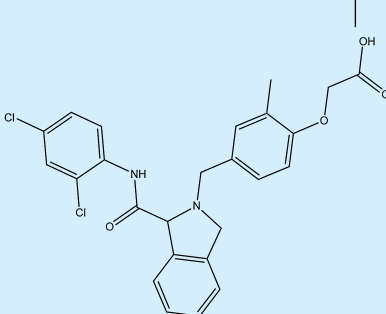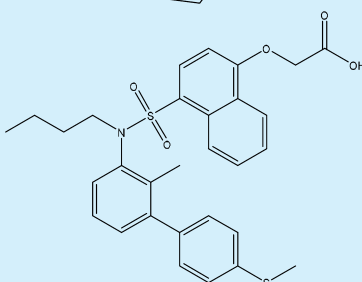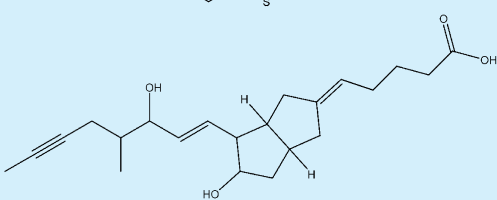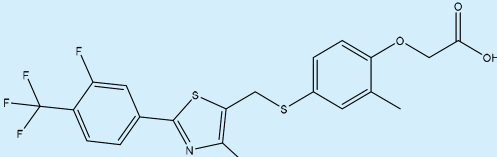
Protein Data Bank code	Ligand structure	EC$_{50}$ (nM)	Reference
3DY6		1259	(Shearer *et al.*, 2008)
3ET2		–	(Artis *et al.*, 2009)
3GWX		4000	(Xu *et al.*, 1999)
3GZ9		54	(Connors *et al.*, 2009)
3OZ0		5	(Luckhurst *et al.*, 2011)
3PEQ		7.4	(Evans *et al.*, 2011)
3SP9		–	(Jin *et al.*, 2011)
3TKM		1.1	(Batista *et al.*, 2012)

Table 2

Comparison of the computational model-based and the *in vitro* assays data on the binding interactions of natural compounds with PPARδ

Compound and *in silico* prediction	Krey *et al.* (1997)	Forman *et al.* (1997)	Xu *et al.* (1999)	Naruhn *et al.* (2010)
ω3-PUFA				
α-Linolenic C18:3[b]	+	+	+	NT
γ-Linolenic C18:3[b]	NT	NT	+	NT
Dihomo-γ-linolenic[b]	NT	NT	+	NT
EPA C20:5[a]	+	+	+	NT
DHA C22:6[b]	+**	+	NT	NT
ω6-PUFA				
Linoleic C18:2[b]	+	+	+	NT
Arachidonic C20:4[b]	+	+	+	NT
ω9-MUFA				
Palmitoleic C16:1[b]	NT	NT	+	NT
Oleic C18:1[a]	+	NT	+	NT
Elaidic C18:1[b]	+	NT	NT	NT
Erucic C22:1[b]	+	NT	–	NT
Nervonic C24:1[b]	+	NT	NT	NT
ω2-MUFA				
Petroselinic C18:1	+	NT	NT	NT
Saturated fatty acids				
Capric C10:0[c]	NT	NT	–	NT
Lauric C12:0[c]	NT	–	–	NT
Myristic C14:0[b]	NT	NT	+	NT
Palmitic C16:0[b]	NT	+**	–	NT
Stearic C18:0[b]	NT	NT	+	NT
Arachidic C20:0[a]	NT	NT	–	NT
Behenic C22:0[b]	NT	NT	–	NT
Dicarboxylic fatty acids				
Dodecanedioic C12[c]	+**	NT	NT	NT
Eicosanoids				
5(S)-HETE[a]	–	NT	NT	NT
5-HpETE[b]	NT	NT	NT	NT
±8-HETE	NT	+	NT	–
8(S)-HETE[b]	+	NT	NT	NT
8(R)-HETE	–	NT	NT	NT
15-HpETE*	NT	NT	NT	+
15(S)HpETE[b]	NT	NT	NT	NT
15(R)HpETE[a]	NT	NT	NT	NT
15(S)-HETE[b]	NT	NT	NT	+
15(R)-HETE[a]	NT	NT	NT	+
12-HpETE[b]	NT	NT	NT	–
±12-HETE[a]	NT	NT	NT	–
LTA$_4$[b]	NT	NT	NT	NT
LTB$_4$[a]	–	NT	NT	NT
LTC$_4$[a]	NT	NT	NT	NT
9(S)-HODE[a]	NT	NT	NT	NT
9(R)-HODE[b]	NT	NT	NT	NT
12-HpODE[b]	NT	NT	NT	NT

Table 2

Continued

Compound and *in silico* prediction	Krey *et al.* (1997)	Forman *et al.* (1997)	Xu *et al.* (1999)	Naruhn *et al.* (2010)
13(S)-HODE[b]	NT	NT	NT	NT
13(R)-HODE[c]	NT	NT	NT	NT
5,15-di-HpETE[b]	NT	NT	NT	NT
5,6-diHETE[a]	NT	NT	NT	NT
Prostaglandins				
PGA$_1$[c]	NT	+	NT	NT
PGA$_2$[b]	NT	+	NT	NT
PGB$_1$[b]	NT	NT	NT	NT
PGB$_2$[b]	NT	+**	NT	NT
PGD$_1$[b]	NT	NT	NT	NT
PGD$_2$[b]	NT	+**	NT	NT
PGD$_3$[b]	NT	NT	NT	NT
PGE$_1$[c]	NT	NT	NT	NT
PGE$_2$[c]	NT	+**	NT	NT
PGE$_3$[c]	NT	NT	NT	NT
PGF$_{1\alpha}$[a]	NT	NT	NT	NT
PGF$_{2\alpha}$[b]	NT	–	NT	NT
PGF$_{3\alpha}$[b]	NT	NT	NT	NT
15d-$\Delta^{12,14}$-PGJ$_2$[c]	+**	–	NT	NT
PGI$_2$[b]	NT	–	NT	NT
Lipoxins				
LXA$_4$[a]	NT	NT	NT	–
LXB$_4$[c]	NT	NT	NT	–
4-Hydroxyalkenals				
4-HpNE[c]	NT	NT	NT	NT
4-HNE[c]	NT	NT	NT	NT
4-HDDE[b]	NT	NT	NT	NT
4-HNA[c]	NT	NT	NT	NT

Sixty two natural ligands out of the 82 database ligands were classified as either [a]PPARδ binders, [b]weak binders or [c]non-binders. NT, not tested.
*Stereoisomers are not indicated in the *in vitro* assays.
**Weak binding.

excluded volumes taken from the complex of the LBD of PPARδ with 5,8,11,14,17-eicosapentaenoic acid (EPA; PDB code 3GWX). The decision to base excluded volumes on a single complex stems from the fact that all PPARδ crystal structures are highly similar. 3GWX was selected for having one of the highest resolutions. Excluded volumes are points in space occupied by protein atoms, which represent steric hindrances in the binding site. Such points cannot be occupied by ligand atoms. In accordance with the binding hypothesis, the final pharmacophore model (Figure 2) is comprised of the H-bond acceptor matching ligand moieties, which are able to form hydrogen bonds with H323/H449/Y473 and two hydrophobic features placed along arm-1 and arm-3, which match the hydrophobic part of the ligands. This pharmacophore successfully recognized 13 out of the 16 known ligands shown in Table 1. A close examination of the

three exceptions, namely 2XYX, 2XYW, 2XYJ, revealed that they share a common sulfonylthiadiazole scaffold and adopt common binding modes within PPARδ, distinct from the binding modes adopted by the other ligands. In particular, these ligands do not form interactions with H323, H449 or Y473 and occupy a lower distal pocket near I213, L219 and W228 that is not filled by the other ligands.

A potential limitation in applying the above-described binding hypothesis to the 82 database ligands is that this model was developed from a set of large ligands (average MW = 481.48), whereas the majority of the database ligands are smaller (averaged MW = 315.61). In order to partially circumvent this difficulty, the hydrophobic features of the pharmacophore model were placed at intermediate rather than at extreme points along arm-2 and arm-3, thereby allowing smaller ligands to fit these features.

Table 3

Comparison of the computational model-based and the *in vitro* assays data on the binding interactions of PPARδ synthetic ligands

| Compound and *in silico* prediction	Krey *et al.* (1997)	Forman *et al.* (1997)
Prostaglandin analogues		
cPGI[b]	NT	+
Iloprost (R)[c]	NT	+*
Iloprost (S)[b]		
Cicaprost[b]	NT	+
Hypolipidaemic agents		
Bezafibrate[b]	+	NT
Ciprofibrate[b]	+	–
Clofibrate[c]	–	+**
Fenofibrate[c]	–	NT
Gemfibrozil[c]	+**	NT
Wy14643[c]	+**	–
ETYA[b]	+	NT
BRL49653[c]	+**	–
Probucol[c]	+**	NT
Nafenopin[b]	+	NT
Other		
2Br-C16[a]	NT	+**
GW501516[a]	NT	NT
TTA[b]	NT	+
Histidine-4-hydroxyhexenal[c]	NT	NT
Histidine-4-hydroxynonenal[c]	NT	NT
Histidine-4-HDDE[c]	NT	NT

Twenty synthetic ligands out of the 82 database ligands classified as either [a]PPARδ binders, [b]weak binders or [c]non-binders. NT, not tested.
*Stereoisomers are not indicated in the article.
**Weak binding.

Effect of histidine protonation states on docking results

In the absence of information (e.g. crystal structures, binding data) on the direct interaction of the 82 database ligands with PPARδ, our analysis had to exclusively rely on results obtained from docking simulations. With this in mind, we started this analysis by evaluating the performances of Glide (Schrödinger, Camberley, UK) (Friesner *et al.*, 2004; Halgren *et al.*, 2004) in terms of its ability to reproduce the 16 crystal structures. Glide is a docking tool aimed at predicting the structures (i.e. binding modes, also known as poses) and energy (i.e. binding free energies) of ligand protein complexes. Flexibly docking the 16 crystallographic ligands into the binding sites of their respective LBDs led to root mean squared deviation (RMSD) values in the range of 0.14–4.78 Å, as the lowest energy poses (except for 3GWX, for which the RMSD was 7.8 Å). RMSD values >2 Å are typically considered unsatisfactory in docking simulations. In order to improve this parameter, we focused our attention on the two histidine
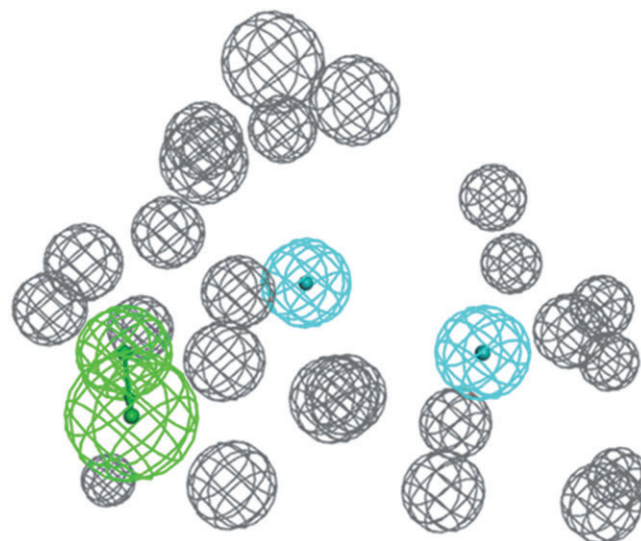
Figure 2

Pharmacophore model, green feature represents the H-bond acceptor matching ligand moieties, which form hydrogen bonds with H323/H449/Y473. Blue features represent the hydrophobic part of the ligands. Grey features represent the excluded volumes.

residues located at the arm-1 of the Y-shaped pocket in the LBD (H323, H449). We assumed that their protonation states could affect the binding modes obtained with Glide. In most crystal structures, both residues form hydrogen bonds with ligand moieties and accordingly were considered to be important for ligand binding. We supposed that the computationally determined protonation states for these residues may depend on the presence of a ligand. This assumption was verified by computationally calculating for each crystal structure the protonation states of H323 and H449 in the presence of its ligand. These calculations were performed by the 'Prepare Protein Protocol' as detailed in the method section of the Supporting Information. Indeed, protonation patterns different from those obtained for the various structures in their ligand-free states were observed. Moreover, repeating the docking procedure for these newly prepared structures led to smaller RMSD values in the range of 0.39–1.15 Å, as the lowest energy poses (again except for 3GWX, with an RMSD value of 7.4 Å). Based on these results, we concluded that the protonation states for H323 and H449 are important for establishing reliable binding modes by the docking simulations.

Docking simulations

Superimposing all 16 PPARδ LBD crystal structures (including 3GWX) available from the PDB (Table 1) revealed only slight differences among them (average RMSD = 0.91 Å), suggesting that they could all be adequately represented by a single structure. This in turn implied that docking of ligands to any of the PPARδ crystal structures should lead to similar binding modes. In order to test this hypothesis, we performed cross-docking simulations, whereby each ligand was docked into all 16 structures and its resulting binding modes were compared with those observed in 'its own' crystal. Prior to docking, the

protonation state of each structure was determined in the presence of its 'native' ligand. Visual inspection revealed that the best results were obtained for the crystal structures of 1GWX and 3GWX (results not shown). Although the RMSD value of 3GWX was high, we tested this structure because of its excellent resolution.

In order to quantify these results, RMSD values between docked and crystal poses were recalculated and averaged across all ligands. These new values were found to be similar for both protein crystal structures (6.1 Å). Because the resolution of 3GWX was slightly better than that of 1GWX (2.4 Å and 2.5 Å, respectively), it was selected for the docking analysis of the other 82 database ligands.

As discussed earlier, the results of the docking simulations for the 16 crystallographic ligands were shown to depend on the protonation states of H323 and H449. To ascertain whether these states could also affect the results obtained for the 82 database ligands, it was important to determine the preferred protonation state of PPARδ LBD. To set a plausible criterion for selecting this state, we assumed that a correct protonation will induce ligand binding in a conformation corresponding to the binding hypothesis. Given Glide's good performances in reproducing the crystal structures of the 16 ligands (Supporting Information Table S1), we further assumed that a large percentage of Glide-generated poses corresponding to the binding hypothesis is indicative of a good PPARδ binder. Multiple protonation states of H323 and H449 were determined in the presence of the 16 crystallographic ligands and of a diverse subset of 10 ligands taken from the database. These ligands were selected based on their structural diversity as manifested in their chemical structures. Structural diversity was assessed by visually inspecting all ligands (see Supporting Information Table S2). Out of a total nine possible combinations of protonation states, only seven were obtained by the 'Prepare Protein Protocol' within Discovery Studio (Accelrys, 2013) (Table 4). 3GWX was protonated according to all seven patterns and used further for docking the 16 ligands. For each protonation state, we then determined the number of the resulting poses that matched the binding hypothesis, as represented by the pharmacophore model. The results (Supporting Information Table S3) demonstrated that docking into a structure in which both histidine moieties were protonated (3GWX_1 in Table 4) produced the largest number of pharmacophore-fitting poses. This structure was therefore selected for docking of the 82 database ligands. Furthermore, for 11 out of the 16 ligands, more than 70% of the poses matched the pharmacophore, which was designed based on our binding hypothesis. According to these data, we hypothesized that PPARδ binders are ligands for which 70% of their Glide-generated poses fit the pharmacophore model.
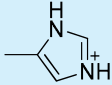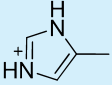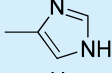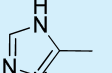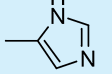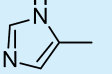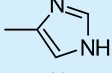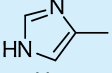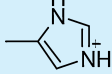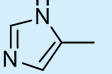
The 82 database ligands were subsequently docked into the 3GWX_1 structure using Glide and the resulting poses were evaluated by the pharmacophore model for their fitness to the binding hypothesis. Using the 70% threshold mentioned earlier, 38 ligands were predicted to bind PPARδ (Supporting Information Table S4).

Quantitative prediction of EC$_{50}$ values

Next, we attempted to develop a quantitative predictor of ligand binding to PPARδ LBD. For this purpose, we studied Glide-generated poses obtained by docking the 16 crystallo-

Table 4

Seven different protonation patterns for the binding site histidine residues H323 and H449
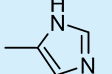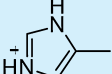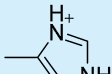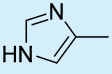

In all cases the ligand is roughly positioned between the two histidine residues. The ligand position is indicated by the blue oval shape.

graphic ligands into the 3GWX structure in its seven protonation states. The first attempt to correlate lowest energy scores with EC$_{50}$ values produced poor results at all protonation states (not shown). In order to achieve better computational estimates of ligand binding-free energies, we selected for each ligand poses matching our binding hypothesis and based on these, estimated its binding-free energy to PPARδ using Equation S1 (See Supporting Information).

Using this approach, a reasonable correlation was obtained for ligand docked into the 3GWX_6 structure ($r^2 = 0.4$ across 11 ligands) (Supporting Information Fig. S1A). No poses matching the binding hypothesis were obtained for ligands 3TKM, 2ZNP, 2ZNQ, 3ET2 and 3SP9 upon docking into the 3GWX_6 structure. This correlation improved to $r^2 = 0.57$ upon removal of a single outlier (2XYJ; see Supporting Information Fig. S1B). Having obtained this correlation, the 82 database ligands were docked into the 3GWX_6 structure, their poses were processed as explained earlier and their EC$_{50}$ values were predicted according to the regression Equation S2 (Supporting Information Fig. S1). Because the least efficacious crystallographic ligands have EC$_{50}$ values in the range of 4 μM (Table 1), we classified ligands with predicted EC$_{50}$ values smaller than this value as potential PPARδ binders. These results are presented in Supporting Information Table S5.

Consensus scoring

Docking simulations based on the pharmacophore model, on the one hand, and the quantification of the docking results

using Equation S1 and the regression Equation S2, on the other, provided two independent predictors (docking-based predictor and regression-based predictor) of ligand binding to PPARδ.

Interestingly, these predictors were developed from docking poses obtained from PPARδ LBD structures that differ in their protonation patterns (3GWX_1 and 3GWX_6). Both structures may represent two states on the potential energy surface of the protein. Because the relative importance of these states is unknown, the most reliable predictor of ligand binding can be potentially obtained by considering a consensus approach in which the binding of each ligand to PPARδ is predicted by the two models. Therefore, we combined the results presented in Supporting Information Tables S4 and S5 into a consensus predictor (Tables 2 and 3). According to this predictor, the 82 ligands are classified to 16 binders (predicted to bind PPARδ LBD by both predictors, denoted by superscript letter a), 42 weak binders (predicted to bind by only one predictor, denoted by superscript letter b) and 24 non-binders (predicted not to bind by both predictors, denoted superscript letter c). This in silico generated prediction data correlated well with the in vitro results of ligand binding and activation of PPARδ, as shown in Tables 2 and 3.

The computer modelling predictions were tested against the experimental data available on 41 different ligands (Table 2). Specifically, ω-3 PUFA [α-linolenic acid, γ-linolenic acid, dihomo-γ-linolenic acid, EPA and docosahexaenoic acid (DHA)], ω-6 PUFA (linoleic acid and arachidonic acid) and MUFA (palmitoleic acid, oleic acid, petroselinic acid, elaidic acid, erucic acid, nervonic acid), which interacted well with the PPARδ LBD in the above-mentioned in vitro binding assays (Forman et al., 1997; Krey et al., 1997; Xu et al., 1999; Naruhn et al., 2010; Jin et al., 2011), were similarly classified by the computational model we developed. Our analysis on the positive binding interaction of erucic acid to the PPARδ LBD agrees with the experimental data obtained by Krey et al. (1997), but not with Xu et al. (1999). The computational model confirms the binding of myristic acid, palmitic acid and stearic acid to the PPARδ LBD (Forman et al., 1997; Xu et al., 1999) and agrees with the lack of significant binding interaction of capric acid and lauric acid (Forman et al., 1997; Xu et al., 1999). However, the computational analyses of the longer saturated arichidic acid and behenic acid deviated from the experimental binding data (Xu et al., 1999). The model successfully identified eicosanoids 8(S)-HETE, 15-HpETE, 15(S)-HETE and 15(R)-HETE as PPARδ LBD binders and also confirmed the lack of binding of 8(R)-HETE (Krey et al., 1997). It is worth noting that while the model predicted good to moderate binding of 5(S)-HETE, 12-HpETE, 12-HETE and LTB$_4$ to PPARδ LBD, the in vitro binding assays failed to detect such binding interactions (Forman et al., 1997; Krey et al., 1997; Naruhn et al., 2010). The binding of prostaglandins to the PPARδ LBD was also evaluated: PGA$_2$, PGB$_2$ and PGD$_2$ that interacted well with the receptor in the in vitro binding assay (Forman et al., 1997) docked well to the LBD in silico (Table 2). The model also predicted the lack of binding of PGE$_2$ and 15d-$\Delta^{12,14}$PGJ$_2$, which indeed failed to bind to PPARδ LBD in the in vitro binding assay (Forman et al., 1997; Krey et al., 1997). Inconsistent with the in vitro binding assays (Forman et al., 1997), our model predicted that PGA$_1$ could not bind and PGI$_2$ could bind to PPARδ LBD. Similar incon-

sistency exited for LXA$_4$, whereas the analysis of LXB$_4$ agreed with the in vitro binding data (Naruhn et al., 2010). Interestingly, our model predicted that the short 4-hydroxyalkenals (4-HpNE, 4-HNE) were not ligands for PPARδ LBD, whereas the longer 4-HDDE was. We reported before that 4-HNE and 4-HDDE activated PPARδ in cell-based assays. The carboxylic derivative of 4-HNE, namely 4-hydroxynonenic acid, which was not active in vitro (Riahi et al., 2010), is not a predicted ligand for PPARδ LBD either.

The potential binding interaction of synthetic compounds with PPARδ LBD was also analysed using the same computational model and compared with the in vitro binding analyses performed independently by Krey et al. and Forman et al. (Forman et al., 1997; Krey et al., 1997). Table 3 shows an excellent correlation for 14 compounds out the 15 that were tested in the in vitro assays and the in silico modelling.

The present computational model, which is based on crystal structures of PPARδ LBD complexes with small synthetic ligands and EPA, independently of in vitro binding assay parameters, shows high degree of correlation to the experimental data on the binding interactions of fatty acids and their metabolites (Table 2): of the 41 different fatty acids and their metabolites that were tested in the different binding assays, our model predicted binding interactions for 28 (68.3%). This correlation increased to 93.3% for the 15 synthetic ligands. Importantly, the 82 database ligands were not used in any way during the model construction phase and consequently constitute a valid external test set. We therefore suggest that the computational model we developed reliably predicts binding interaction of natural and synthetic ligands to the recombinant PPARδ LBD and may therefore assist in planning and performing complex in vitro binding assay, while mitigating the risk of testing inactive compounds.

As all computational models, the current one also suffers from several limitations. Some of these limitations are common to most pharmacophore-based and docking-based models. Such models focus on predicting binding affinities (or binding trends) of ligand–protein complexes rather than the downstream outcome of the binding event (e.g. activation). Moreover, binding is often equated with simple scoring function, which typically only considers ligand binding site interactions and neglects important contributions from desolvation, loss of entropy (translational, rotational and vibrational) and conformational changes (resulting from the energy required by both ligand and protein to attain their bioactive conformations). Thus, the present model is confounded by the same limitations of the in vitro binding assays, which poorly predict or correlate to cell-based activation of PPARδ by natural or synthetic ligands. Therefore, further analysis of potential PPARδ ligands based on this model requires confirmation in a cell-based activation assay of PPARδ. Forman et al. show clearly the lack of a correlation between the ability of ligands to bind to recombinant LBD of the various PPAR and the degree of the activation of the receptor in cells (Forman et al., 1997). For example, 15d-PGJ$_2$ did not bind to PPARδ LBD but activated the receptor in the PPARδ-based transactivation assay14-fold. Conversely, PGD$_2$ and DHA that negligibly bound to PPARδ LBD activated the receptor fourfold and sixfold respectively.

Several explanations for these discrepancies can be proposed. For instance, the allosteric activation and induced

conformational changes in PPARδ may modulate its interactions with its cognate partners (RXR, co-activators and DNA-containing PPRE sequences); a similar modulation in RXR can also enhance or limit its ability to dimerize and interact with PPRE. Moreover, the dimer PPARδ-RXR may allosterically assume different conformations that reduce or increase the binding affinity of co-activators or co-repressors, and thus affect its capacity to assemble an active transcriptional complex (Zoete *et al.*, 2007). It has been shown that ligand binding to many transcription factors, including PPARs and steroid receptors, induces conformational changes in distant domains of the proteins or their cognate dimerization partners (Nolte *et al.*, 1998; Gampe *et al.*, 2000; Lu *et al.*, 2008). For instance, Venalainen *et al.* suggested that ligand binding to RXRα (also known as NR2B1) in its complex with PPARα induced conformation changes in the latter's helix 8–9 loop within the heterodimerization interface and in helices 3 and 4 at the co-activator binding site, contributing to the stabilization of the heterodimer and its complex with co-activators (Venalainen *et al.*, 2010). Several studies have suggested that ligand binding to PPARs resulted in a more compact and rigid structure to the LBD (Johnson *et al.*, 2000; Cronet *et al.*, 2001; Berger *et al.*, 2003). It has been proposed that the binding of co-activators to PPARs requires allosteric modifications in the AF-2 helical domain in the receptor dimer, followed by conformational changes in a hydrophobic cleft on the surface of the receptor (Johnson *et al.*, 2000). Nonetheless, models based solely on recombinant PPARδ-LBD crystals with various ligands are not useful for the analysis of conformational changes induced by ligand binding to PPARδ or PPARδ-RXR dimers. In the absence of whole receptor or whole-dimer crystals, a partial understanding of these complex allosteric modulations may be deduced from analysis of co-crystals of LBD of PPARs and RXR with co-activator proteins. Some studies on such co-crystals suggest that the binding interactions of co-activators with the receptor were enhanced by an allosteric interaction in the AF-2 helical domain (Johnson *et al.*, 2000; Cronet *et al.*, 2001; Sznaidman *et al.*, 2003; Ostberg *et al.*, 2004; Xu *et al.*, 2004; Burgermeister *et al.*, 2006). Theoretical and practical modelling of PPAR activation should also take into consideration recent findings on the involvement of side chains of highly conserved amino acids that stabilize helix 12 of the LBD and induce ligand-independent activation of the receptor (Zoete *et al.*, 2007).

Many of the proposed PPARδ endogenous activators are fatty acid and fatty acid metabolites, which are substrates of various enzymatic and non-enzymatic pathways that generate numerous lipid-derived mediators (e.g. PGs, lipoxins, HETEs, EETs, oxidized fatty acids, 4-hydroxyalkenals, oxo-alkenals) (Yoda and Okazaki, 1991; Cohen *et al.*, 2011a; Massey and Nicolaou, 2011; Murakami, 2011; Catala, 2013; Walley *et al.*, 2013). The assumption that these fatty acids, and their derivatives and metabolites, directly activate PPARs in cells requires a careful examination. For instance, our previous studies suggested that the non-enzymatic peroxidation products of arachidonic acid, namely 4-HDDE and 4-HNE activated PPARδ in vascular endothelial cells and insulin secreting β-cells (Riahi *et al.*, 2010; Cohen *et al.*, 2011b). Yet the current computational model predicts the binding of 4-HDDE, but not 4-HNE to PPARδ LBD. This disparity may result from further metabolism of these molecules to direct ligands of PPARδ. Similarly, these metabolites may also function as allosteric modulators of PPARδ or PPARδ-RXR dimers and enhance the binding of endogenous ligands or co-activators with the receptor.

In summary, the computational chemistry approach we propose to predict and analyse binding interactions of ligands with the PPARδ-LBD is highly suitable for synthetic ligands. Although this approach exhibits a high degree of prediction of positive binding interactions of natural activators with the LBD, it is not yet ideal, because of the complexity of ligand binding and ligand-induced conformational and allosteric changes in PPARδ and PPARδ-RXR dimers and the lack of crystals for the whole PPARδ and PPARδ-RXR dimer. Potential improvements to the model therefore include the introduction of conformational flexibility via molecular dynamic simulations. Alternatively, statistical modelling approaches (e.g. quantitative structure-activity relationship) could be employed using activation data as the independent variable to build predictive models. Such approaches, however, require a large database (e.g. >100 compounds). Nevertheless, the present *in silico* modelling may be useful for designing potent and selective PPARδ ligands without relying solely on PPARδ-LBD crystallographic analysis. Moreover, the model may prove useful in the search for natural and synthetic activators of PPARδ.

Acknowledgements

Conflict of interest

The authors have no conflicts to report.

References

Accelrys (2013). Accelrys Software Inc., Discovery Studio Modeling Environment, Release 4.0. Accelrys Software Inc: San Diego.

Alexander SPH, Benson HE, Faccenda E, Pawson AJ, Sharman JL, Spedding M *et al.* (2013). The Concise Guide to PHARMACOLOGY 2013/14: Nuclear hormone receptors. Br J Pharmacol. 170: 1652–1675.

Anbalagan M, Huderson B, Murphy L, Rowan BG (2012). Post-translational modifications of nuclear receptors and human disease. Nucl Recept Signal 10: e001.

Arsenijevic D, de Bilbao F, Plamondon J, Paradis E, Vallet P, Richard D et al. (2006). Increased infarct size and lack of hyperphagic response after focal cerebral ischemia in peroxisome proliferator-activated receptor beta-deficient mice. J Cereb Blood Flow Metab 26: 433–445.

Artis DR, Lin JJ, Zhang C, Wang W, Mehra U, Perreault M et al. (2009). Scaffold-based discovery of indeglitazar, a PPAR pan-active anti-diabetic agent. Proc Natl Acad Sci U S A 106: 262–267.

Astapova O, Leff T (2012). Adiponectin and PPARγ: cooperative and interdependent actions of two key regulators of metabolism. Vitam Horm 90: 143–162.

Barak Y, Liao D, He W, Ong ES, Nelson MC, Olefsky JM et al. (2002). Effects of peroxisome proliferator-activated receptor delta on placentation, adiposity, and colorectal cancer. Proc Natl Acad Sci U S A 99: 303–308.

Barish GD, Atkins AR, Downes M, Olson P, Chong LW, Nelson M et al. (2008). PPARdelta regulates multiple proinflammatory pathways to suppress atherosclerosis. Proc Natl Acad Sci U S A 105: 4271–4276.

Barroso E, del Valle J, Porquet D, Vieira Santos AM, Salvado L, Rodriguez-Rodriguez R et al. (2013). Tau hyperphosphorylation and increased BACE1 and RAGE levels in the cortex of PPARβ/δ-null mice. Biochim Biophys Acta 1832: 1241–1248.

Batista FA, Trivella DB, Bernardes A, Gratieri J, Oliveira PS, Figueira AC et al. (2012). Structural insights into human peroxisome proliferator activated receptor delta (PPAR-delta) selective ligand binding. PLoS ONE 7: e33643.

Benetti E, Patel NS, Collino M (2011). The role of PPARβ/δ in the management of metabolic syndrome and its associated cardiovascular complications. Endocr Metab Immune Disord Drug Targets 11: 273–284.

Berger JP, Petro AE, Macnaul KL, Kelly LJ, Zhang BB, Richards K et al. (2003). Distinct properties and advantages of a novel peroxisome proliferator-activated protein [gamma] selective modulator. Mol Endocrinol 17: 662–676.

Bourguet W, Ruff M, Chambon P, Gronemeyer H, Moras D (1995). Crystal structure of the ligand-binding domain of the human nuclear receptor RXR-alpha. Nature 375: 377–382.

Burdick AD, Kim DJ, Peraza MA, Gonzalez FJ, Peters JM (2006). The role of peroxisome proliferator-activated receptor-beta/delta in epithelial cell growth and differentiation. Cell Signal 18: 9–20.

Burgermeister E, Schnoebelen A, Flament A, Benz J, Stihle M, Gsell B et al. (2006). A novel partial agonist of peroxisome proliferator-activated receptor-gamma (PPARgamma) recruits PPARgamma-coactivator-1alpha, prevents triglyceride accumulation, and potentiates insulin signaling in vitro. Mol Endocrinol 20: 809–830.

Carrieri A, Giudici M, Parente M, De Rosas M, Piemontese L, Fracchiolla G et al. (2013). Molecular determinants for nuclear receptors selectivity: chemometric analysis, dockings and site-directed mutagenesis of dual peroxisome proliferator-activated receptors α/γ agonists. Eur J Med Chem 63: 321–332.

Catala A (2013). Five decades with polyunsaturated fatty acids: chemical synthesis, enzymatic formation, lipid peroxidation and its biological effects. J Lipids 2013: 710290.

Chandra V, Huang P, Hamuro Y, Raghuram S, Wang Y, Burris TP et al. (2008). Structure of the intact PPAR-gamma-RXR-nuclear receptor complex on DNA. Nature 456: 350–356.

Chen W, Wang LL, Liu HY, Long L, Li S (2008). Peroxisome proliferator-activated receptor delta-agonist, GW501516,

ameliorates insulin resistance, improves dyslipidaemia in monosodium L-glutamate metabolic syndrome mice. Basic Clin Pharmacol Toxicol 103: 240–246.

Clinckemalie L, Vanderschueren D, Boonen S, Claessens F (2012). The hinge region in androgen receptor control. Mol Cell Endocrinol 358: 1–8.

Cohen G, Riahi Y, Sasson S (2011a). Lipid peroxidation of poly-unsaturated fatty acids in normal and obese adipose tissues. Arch Physiol Biochem 117: 131–139.

Cohen G, Riahi Y, Shamni O, Guichardant M, Chatgilialoglu C, Ferreri C et al. (2011b). Role of lipid peroxidation and PPAR-δ in amplifying glucose-stimulated insulin secretion. Diabetes 60: 2830–2842.

Cohen G, Riahi Y, Sunda V, Deplano S, Chatgilialoglu C, Ferreri C et al. (2013). Signaling properties of 4-hydroxyalkenals formed by lipid peroxidation in diabetes. Free Radic Biol Med 65: 978–987.

Coleman JD, Prabhu KS, Thompson JT, Reddy PS, Peters JM, Peterson BR et al. (2007). The oxidative stress mediator 4-hydroxynonenal is an intracellular agonist of the nuclear receptor peroxisome proliferator-activated receptor-beta/delta (PPARbeta/delta). Free Radic Biol Med 42: 1155–1164.

Coll T, Rodriguez-Calvo R, Barroso E, Serrano L, Eyre E, Palomer X et al. (2009). Peroxisome proliferator-activated receptor (PPAR) beta/delta: a new potential therapeutic target for the treatment of metabolic syndrome. Curr Mol Pharmacol 2: 46–55.

Connors RV, Wang Z, Harrison M, Zhang A, Wanska M, Hiscock S et al. (2009). Identification of a PPARdelta agonist with partial agonistic activity on PPARgamma. Bioorg Med Chem Lett 19: 3550–3554.

Cronet P, Petersen JF, Folmer R, Blomberg N, Sjoblom K, Karlsson U et al. (2001). Structure of the PPARalpha and -gamma ligand binding domain in complex with AZ 242; ligand selectivity and agonist activation in the PPAR family. Structure 9: 699–706.

Dressel U, Allen TL, Pippal JB, Rohde PR, Lau P, Muscat GE (2003). The peroxisome proliferator-activated receptor beta/delta agonist, GW501516, regulates the expression of genes involved in lipid catabolism and energy uncoupling in skeletal muscle cells. Mol Endocrinol 17: 2477–2493.

Dreyer C, Keller H, Mahfoudi A, Laudet V, Krey G, Wahli W (1993). Positive regulation of the peroxisomal beta-oxidation pathway by fatty acids through activation of peroxisome proliferator-activated receptors (PPAR). Biol Cell 77: 67–76.

de Duve D (1969). The peroxisome: a new cytoplasmic organelle. Proc R Soc Lond B Biol Sci 173: 71–83.

Ebdrup S, Pettersson I, Rasmussen HB, Deussen HJ, Frost Jensen A, Mortensen SB et al. (2003). Synthesis and biological and structural characterization of the dual-acting peroxisome proliferator-activated receptor alpha/gamma agonist ragaglitazar. J Med Chem 46: 1306–1317.

Ehrenborg E, Krook A (2009). Regulation of skeletal muscle physiology and metabolism by peroxisome proliferator-activated receptor delta. Pharmacol Rev 61: 373–393.

Ehrenborg E, Skogsberg J (2013). Peroxisome proliferator-activated receptor delta and cardiovascular disease. Atherosclerosis 231: 95–106.

Evans KA, Shearer BG, Wisnoski DD, Shi D, Sparks SM, Sternbach DD et al. (2011). Phenoxyacetic acids as PPARδ partial agonists: synthesis, optimization, and in vivo efficacy. Bioorg Med Chem Lett 21: 2345–2350.

Fan Y, Wang Y, Tang Z, Zhang H, Qin X, Zhu Y et al. (2008). Suppression of pro-inflammatory adhesion molecules by PPAR-delta in human vascular endothelial cells. Arterioscler Thromb Vasc Biol 28: 315–321.

Forman BM, Chen J, Evans RM (1997). Hypolipidemic drugs, polyunsaturated fatty acids, and eicosanoids are ligands for peroxisome proliferator-activated receptors alpha and delta. Proc Natl Acad Sci U S A 94: 4312–4317.

Friesner RA, Banks JL, Murphy RB, Halgren TA, Klicic JJ, Mainz DT et al. (2004). Glide: a new approach for rapid, accurate docking and scoring. 1. Method and assessment of docking accuracy. J Med Chem 47: 1739–1749.

Fyffe SA, Alphey MS, Buetow L, Smith TK, Ferguson MA, Sorensen MD et al. (2006). Recombinant human PPAR-beta/delta ligand-binding domain is locked in an activated conformation by endogenous fatty acids. J Mol Biol 356: 1005–1013.

Gampe RT Jr, Montana VG, Lambert MH, Miller AB, Bledsoe RK, Milburn MV et al. (2000). Asymmetry in the PPARgamma/RXRalpha crystal structure reveals the molecular basis of heterodimerization among nuclear receptors. Mol Cell 5: 545–555.

Gupta RA, Wang D, Katkuri S, Wang H, Dey SK, DuBois RN (2004). Activation of nuclear hormone receptor peroxisome proliferator-activated receptor-delta accelerates intestinal adenoma growth. Nat Med 10: 245–247.

Halgren TA, Murphy RB, Friesner RA, Beard HS, Frye LL, Pollard WT et al. (2004). Glide: a new approach for rapid, accurate docking and scoring. 2. Enrichment factors in database screening. J Med Chem 47: 1750–1759.

Hallenbeck PL, Marks MS, Lippoldt RE, Ozato K, Nikodem VM (1992). Heterodimerization of thyroid hormone (TH) receptor with H-2RIIBP (RXR beta) enhances DNA binding and TH-dependent transcriptional activation. Proc Natl Acad Sci U S A 89: 5572–5576.

Hansen JB, Zhang H, Rasmussen TH, Petersen RK, Flindt EN, Kristiansen K (2001). Peroxisome proliferator-activated receptor delta (PPARdelta)-mediated regulation of preadipocyte proliferation and gene expression is dependent on cAMP signaling. J Biol Chem 276: 3175–3182.

Helsen C, Claessens F (2014). Looking at nuclear receptors from a new angle. Mol Cell Endocrinol 382: 97–106.

Hsu MH, Palmer CN, Song W, Griffin KJ, Johnson EF (1998). A carboxyl-terminal extension of the zinc finger domain contributes to the specificity and polarity of peroxisome proliferator-activated receptor DNA binding. J Biol Chem 273: 27988–27997.

Huang JC, Wun WS, Goldsby JS, Wun IC, Noorhasan D, Wu KK (2007). Stimulation of embryo hatching and implantation by prostacyclin and peroxisome proliferator-activated receptor delta activation: implication in IVF. Hum Reprod 22: 807–814.

Issemann I, Green S (1990). Activation of a member of the steroid hormone receptor superfamily by peroxisome proliferators. Nature 347: 645–650.

Iwashita A, Muramatsu Y, Yamazaki T, Muramoto M, Kita Y, Yamazaki S et al. (2007). Neuroprotective efficacy of the peroxisome proliferator-activated receptor delta-selective agonists in vitro and in vivo. J Pharmacol Exp Ther 320: 1087–1096.

Iwata Y, Miyamoto S, Takamura M, Yanagisawa H, Kasuya A (2001). Interaction between peroxisome proliferator-activated receptor gamma and its agonists: docking study of oximes having 5-benzyl-2,4-thiazolidinedione. J Mol Graph Model 19: 536–542.

Jehl-Pietri C, Bastie C, Gillot I, Luquet S, Grimaldi PA (2000). Peroxisome-proliferator-activated receptor delta mediates the effects of long-chain fatty acids on post-confluent cell proliferation. Biochem J 350 (Pt 1): 93–98.

Jiang B, Liang P, Zhang B, Song J, Huang X, Xiao X (2009). Role of PPAR-beta in hydrogen peroxide-induced apoptosis in human umbilical vein endothelial cells. Atherosclerosis 204: 353–358.

Jin L, Lin S, Rong H, Zheng S, Jin S, Wang R et al. (2011). Structural basis for iloprost as a dual peroxisome proliferator-activated receptor alpha/delta agonist. J Biol Chem 286: 31473–31479.

Johnson BA, Wilson EM, Li Y, Moller DE, Smith RG, Zhou G (2000). Ligand-induced stabilization of PPARgamma monitored by NMR spectroscopy: implications for nuclear receptor activation. J Mol Biol 298: 187–194.

Kalinin S, Richardson JC, Feinstein DL (2009). A PPARdelta agonist reduces amyloid burden and brain inflammation in a transgenic mouse model of Alzheimer's disease. Curr Alzheimer Res 6: 431–437.

Kallenberger BC, Love JD, Chatterjee VK, Schwabe JW (2003). A dynamic mechanism of nuclear receptor activation and its perturbation in a human disease. Nat Struct Biol 10: 136–140.

Keil S, Matter H, Schonafinger K, Glien M, Mathieu M, Marquette JP et al. (2011). Sulfonylthiadiazoles with an unusual binding mode as partial dual peroxisome proliferator-activated receptor (PPAR) γ/δ agonists with high potency and in vivo efficacy. ChemMedChem 6: 633–653.

Krey G, Braissant O, L'Horset F, Kalkhoven E, Perroud M, Parker MG et al. (1997). Fatty acids, eicosanoids, and hypolipidemic agents identified as ligands of peroxisome proliferator-activated receptors by coactivator-dependent receptor ligand assay. Mol Endocrinol 11: 779–791.

Kumar R, Thompson EB (1999). The structure of the nuclear hormone receptors. Steroids 64: 310–319.

Lee CH, Olson P, Hevener A, Mehl I, Chong LW, Olefsky JM et al. (2006). PPARdelta regulates glucose metabolism and insulin sensitivity. Proc Natl Acad Sci U S A 103: 3444–3449.

Lee MY, Lee YJ, Kim YH, Lee SH, Park JH, Kim MO et al. (2009). Role of peroxisome proliferator-activated receptor (PPAR)δ in embryonic stem cell proliferation. Int J Stem Cells 2: 28–34.

Liang YJ, Liu YC, Chen CY, Lai LP, Shyu KG, Juang SJ et al. (2010). Comparison of PPARδ and PPARγ in inhibiting the pro-inflammatory effects of C-reactive protein in endothelial cells. Int J Cardiol 143: 361–367.

Lim H, Gupta RA, Ma WG, Paria BC, Moller DE, Morrow JD et al. (1999). Cyclo-oxygenase-2-derived prostacyclin mediates embryo implantation in the mouse via PPARdelta. Genes Dev 13: 1561–1574.

Lu J, Chen M, Stanley SE, Li E (2008). Effect of heterodimer partner RXRalpha on PPARgamma activation function-2 helix in solution. Biochem Biophys Res Commun 365: 42–46.

Luckhurst CA, Stein LA, Furber M, Webb N, Ratcliffe MJ, Allenby G et al. (2011). Discovery of isoindoline and tetrahydroisoquinoline derivatives as potent, selective PPARδ agonists. Bioorg Med Chem Lett 21: 492–496.

Luquet S, Lopez-Soriano J, Holst D, Fredenrich A, Melki J, Rassoulzadegan M et al. (2003). Peroxisome proliferator-activated receptor delta controls muscle development and oxidative capability. FASEB J 17: 2299–2301.

Martin HL, Mounsey RB, Sathe K, Mustafa S, Nelson MC, Evans RM et al. (2013). A peroxisome proliferator-activated receptor-δ agonist provides neuroprotection in the 1-methyl-4-phenyl-1,2,3,6-tetrahydropyridine model of Parkinson's disease. Neuroscience 240: 191–203.

Massey KA, Nicolaou A (2011). Lipidomics of polyunsaturated-fatty-acid-derived oxygenated metabolites. Biochem Soc Trans 39: 1240–1246.

Michalik L, Desvergne B, Tan NS, Basu-Modak S, Escher P, Rieusset J et al. (2001). Impaired skin wound healing in peroxisome proliferator-activated receptor (PPAR)alpha and PPARbeta mutant mice. J Cell Biol 154: 799–814.

Murakami M (2011). Lipid mediators in life science. Exp Anim 60: 7–20.

Naruhn S, Meissner W, Adhikary T, Kaddatz K, Klein T, Watzer B et al. (2010). 15-hydroxyeicosatetraenoic acid is a preferential peroxisome proliferator-activated receptor beta/delta agonist. Mol Pharmacol 77: 171–184.

Nolte RT, Wisely GB, Westin S, Cobb JE, Lambert MH, Kurokawa R et al. (1998). Ligand binding and co-activator assembly of the peroxisome proliferator-activated receptor-gamma. Nature 395: 137–143.

Okuno M, Arimoto E, Ikenobu Y, Nishihara T, Imagawa M (2001). Dual DNA-binding specificity of peroxisome-proliferator-activated receptor gamma controlled by heterodimer formation with retinoid X receptor alpha. Biochem J 353 (Pt 2): 193–198.

Oliver WR Jr, Shenk JL, Snaith MR, Russell CS, Plunket KD, Bodkin NL et al. (2001). A selective peroxisome proliferator-activated receptor delta agonist promotes reverse cholesterol transport. Proc Natl Acad Sci U S A 98: 5306–5311.

Ostberg T, Svensson S, Selen G, Uppenberg J, Thor M, Sundbom M et al. (2004). A new class of peroxisome proliferator-activated receptor agonists with a novel binding epitope shows antidiabetic effects. J Biol Chem 279: 41124–41130.

Oyama T, Toyota K, Waku T, Hirakawa Y, Nagasawa N, Kasuga JI et al. (2009). Adaptability and selectivity of human peroxisome proliferator-activated receptor (PPAR) pan agonists revealed from crystal structures. Acta Crystallogr D Biol Crystallogr 65 (Pt 8): 786–795.

Paterniti I, Esposito E, Mazzon E, Galuppo M, Di Paola R, Bramanti P et al. (2010). Evidence for the role of peroxisome proliferator-activated receptor-beta/delta in the development of spinal cord injury. J Pharmacol Exp Ther 333: 465–477.

Pawson AJ, Sharman JL, Benson HE, Faccenda E, Alexander SP, Buneman OP et al.; NC-IUPHAR (2014). The IUPHAR/BPS Guide to PHARMACOLOGY: an expert-driven knowledgebase of drug targets and their ligands. Nucl. Acids Res. 42 (Database Issue): D1098–106.

Peters JM, Lee SS, Li W, Ward JM, Gavrilova O, Everett C et al. (2000). Growth, adipose, brain, and skin alterations resulting from targeted disruption of the mouse peroxisome proliferator-activated receptor beta(delta). Mol Cell Biol 20: 5119–5128.

Pettersson I, Ebdrup S, Havranek M, Pihera P, Korinek M, Mogensen JP et al. (2007). Design of a partial PPARdelta agonist. Bioorg Med Chem Lett 17: 4625–4629.

Pialat JB, Cho TH, Beuf O, Joye E, Moucharrafie S, Langlois JB et al. (2007). MRI monitoring of focal cerebral ischemia in peroxisome proliferator-activated receptor (PPAR)-deficient mice. NMR Biomed 20: 335–342.

Piqueras L, Sanz MJ, Perretti M, Morcillo E, Norling L, Mitchell JA et al. (2009). Activation of PPARbeta/delta inhibits leukocyte recruitment, cell adhesion molecule expression, and chemokine release. J Leukoc Biol 86: 115–122.

Polak PE, Kalinin S, Dello Russo C, Gavrilyuk V, Sharp A, Peters JM et al. (2005). Protective effects of a peroxisome proliferator-activated

receptor-beta/delta agonist in experimental autoimmune encephalomyelitis. J Neuroimmunol 168: 65–75.

Pyper SR, Viswakarma N, Yu S, Reddy JK (2010). PPARalpha: energy combustion, hypolipidemia, inflammation and cancer. Nucl Recept Signal 8: e002.

Renaud JP, Rochel N, Ruff M, Vivat V, Chambon P, Gronemeyer H et al. (1995). Crystal structure of the RAR-gamma ligand-binding domain bound to all-trans retinoic acid. Nature 378: 681–689.

Riahi Y, Sin-Malia Y, Cohen G, Alpert E, Gruzman A, Eckel J et al. (2010). The natural protective mechanism against hyperglycemia in vascular endothelial cells: roles of the lipid peroxidation product 4-hydroxydodecadienal and peroxisome proliferator-activated receptor delta. Diabetes 59: 808–818.

Riserus U, Sprecher D, Johnson T, Olson E, Hirschberg S, Liu A et al. (2008). Activation of peroxisome proliferator-activated receptor (PPAR)delta promotes reversal of multiple metabolic abnormalities, reduces oxidative stress, and increases fatty acid oxidation in moderately obese men. Diabetes 57: 332–339.

Rival Y, Beneteau N, Taillandier T, Pezet M, Dupont-Passelaigue E, Patoiseau JF et al. (2002). PPARalpha and PPARdelta activators inhibit cytokine-induced nuclear translocation of NF-kappaB and expression of VCAM-1 in EAhy926 endothelial cells. Eur J Pharmacol 435: 143–151.

Roemer SC, Donham DC, Sherman L, Pon VH, Edwards DP, Churchill ME (2006). Structure of the progesterone receptor-deoxyribonucleic acid complex: novel interactions required for binding to half-site response elements. Mol Endocrinol 20: 3042–3052.

Schmidt A, Endo N, Rutledge SJ, Vogel R, Shinar D, Rodan GA (1992). Identification of a new member of the steroid hormone receptor superfamily that is activated by a peroxisome proliferator and fatty acids. Mol Endocrinol 6: 1634–1641.

Shaffer PL, Gewirth DT (2002). Structural basis of VDR-DNA interactions on direct repeat response elements. EMBO J 21: 2242–2252.

Shearer BG, Patel HS, Billin AN, Way JM, Winegar DA, Lambert MH et al. (2008). Discovery of a novel class of PPARdelta partial agonists. Bioorg Med Chem Lett 18: 5018–5022.

Skerrett R, Malm T, Landreth G (2014). Nuclear receptors in neurodegenerative diseases. Neurobiol Dis 72: 104–116.

Sprecher DL, Massien C, Pearce G, Billin AN, Perlstein I, Willson TM et al. (2007). Triglyceride:high-density lipoprotein cholesterol effects in healthy subjects administered a peroxisome proliferator activated receptor delta agonist. Arterioscler Thromb Vasc Biol 27: 359–365.

Sznaidman ML, Haffner CD, Maloney PR, Fivush A, Chao E, Goreham D et al. (2003). Novel selective small molecule agonists for peroxisome proliferator-activated receptor delta (PPARdelta) – synthesis and biological activity. Bioorg Med Chem Lett 13: 1517–1521.

Tanaka T, Yamamoto J, Iwasaki S, Asaba H, Hamura H, Ikeda Y et al. (2003). Activation of peroxisome proliferator-activated receptor delta induces fatty acid beta-oxidation in skeletal muscle and attenuates metabolic syndrome. Proc Natl Acad Sci U S A 100: 15924–15929.

Thulin P, Glinghammar B, Skogsberg J, Lundell K, Ehrenborg E (2008). PPARdelta increases expression of the human apolipoprotein A-II gene in human liver cells. Int J Mol Med 21: 819–824.

van der Veen JN, Kruit JK, Havinga R, Baller JF, Chimini G, Lestavel S *et al.* (2005). Reduced cholesterol absorption upon PPARdelta activation coincides with decreased intestinal expression of NPC1L1. J Lipid Res 46: 526–534.

Venalainen T, Molnar F, Oostenbrink C, Carlberg C, Perakyla M (2010). Molecular mechanism of allosteric communication in the human PPARalpha-RXRalpha heterodimer. Proteins 78: 873–887.

Wagner KD, Wagner N (2010). Peroxisome proliferator-activated receptor beta/delta (PPARbeta/delta) acts as regulator of metabolism linked to multiple cellular functions. Pharmacol Ther 125: 423–435.

Wahli W, Michalik L (2012). PPARs at the crossroads of lipid signaling and inflammation. Trends Endocrinol Metab 23: 351–363.

Wallace JM, Schwarz M, Coward P, Houze J, Sawyer JK, Kelley KL *et al.* (2005). Effects of peroxisome proliferator-activated receptor alpha/delta agonists on HDL-cholesterol in vervet monkeys. J Lipid Res 46: 1009–1016.

Walley JW, Kliebenstein DJ, Bostock RM, Dehesh K (2013). Fatty acids and early detection of pathogens. Curr Opin Plant Biol 16: 520–526.

Wang YX, Lee CH, Tiep S, Yu RT, Ham J, Kang H *et al.* (2003). Peroxisome-proliferator-activated receptor delta activates fat metabolism to prevent obesity. Cell 113: 159–170.

Wang YX, Zhang CL, Yu RT, Cho HK, Nelson MC, Bayuga-Ocampo CR *et al.* (2004). Regulation of muscle fiber type and running endurance by PPARdelta. PLoS Biol 2: e294.

Wolf G (2010). Retinoic acid activation of peroxisome proliferation-activated receptor delta represses obesity and insulin resistance. Nutr Rev 68: 67–70.

Xu HE, Lambert MH, Montana VG, Parks DJ, Blanchard SG, Brown PJ *et al.* (1999). Molecular recognition of fatty acids by peroxisome proliferator-activated receptors. Mol Cell 3: 397–403.

Xu HE, Lambert MH, Montana VG, Plunket KD, Moore LB, Collins JL *et al.* (2001). Structural determinants of ligand binding selectivity between the peroxisome proliferator-activated receptors. Proc Natl Acad Sci U S A 98: 13919–13924.

Xu RX, Lambert MH, Wisely BB, Warren EN, Weinert EE, Waitt GM *et al.* (2004). A structural basis for constitutive activity in the human CAR/RXRalpha heterodimer. Mol Cell 16: 919–928.

Yin KJ, Deng Z, Hamblin M, Xiang Y, Huang H, Zhang J *et al.* (2010). Peroxisome proliferator-activated receptor delta regulation of miR-15a in ischemia-induced cerebral vascular endothelial injury. J Neurosci 30: 6398–6408.

Yoda K, Okazaki T (1991). Specificity of recognition sequence for *Escherichia coli* primase. Mol Gen Genet 227: 1–8.

Yu K, Bayona W, Kallen CB, Harding HP, Ravera CP, McMahon G *et al.* (1995). Differential activation of peroxisome proliferator-activated receptors by eicosanoids. J Biol Chem 270: 23975–23983.

Zhang J, Fu M, Zhu X, Xiao Y, Mou Y, Zheng H *et al.* (2002). Peroxisome proliferator-activated receptor delta is up-regulated during vascular lesion formation and promotes post-confluent cell proliferation in vascular smooth muscle cells. J Biol Chem 277: 11505–11512.

Zieleniak A, Wojcik M, Wozniak LA (2008). Structure and physiological functions of the human peroxisome proliferator-activated receptor gamma. Arch Immunol Ther Exp (Warsz) 56: 331–345.

Zoete V, Grosdidier A, Michielin O (2007). Peroxisome proliferator-activated receptor structures: ligand specificity, molecular switch and interactions with regulators. Biochim Biophys Acta 1771: 915–925.

Supporting information

Additional Supporting Information may be found in the online version of this article at the publisher's web-site:

http://dx.doi.org/10.1111/bph.12950

Figure S1 Experimentally determined EC_{50} values.

Table S1 RMSD values for the lowest energy Glide-generated poses with respect to the crystal structures for the 16 crystallographic ligands.

Table S2 Ten structurally diverse ligands selected for the analysis of H323 and H449 protonation states.

Table S3 Docking results obtained for the 16 crystallographic ligands to the seven protonation states of PPARδ LBD (PDB code 3GWX).

Table S4 Docking results for the 82 database ligands into the 3GWX_1 crystal structure. Each entry gives the fraction of poses matching the binding hypothesis from among all poses.

Table S5 Predicted EC_{50} values for 38 out of the 82 database ligands calculated according to regression Equation S2. Ligands for which no binding modes matching the binding hypothesis were identified were not considered.

Table S6 Approximated binding free energies calculation for 38 out of 82 database ligands according to Equation S1.

Appendix S1 Methods used for the molecular modelling.